HAL open science

Synthesis and characterization of polymethine dyes carrying thiobarbituric and carboxylic acid moieties

Arthur Desvals, Mariagrazia Fortino, Corentin Lefebvre, Johann Rogier, Clément Michelin, Samy Alioui, Elodie Rousset, Alfonso Pedone, Gilles Lemercier, Norbert Hoffmann

To cite this version:

Arthur Desvals, Mariagrazia Fortino, Corentin Lefebvre, Johann Rogier, Clément Michelin, et al.. Synthesis and characterization of polymethine dyes carrying thiobarbituric and carboxylic acid moieties. New Journal of Chemistry, 2022, 10.1039/D2NJ00684G . hal-03653553v2

HAL Id: hal-03653553

https://hal.science/hal-03653553v2

Submitted on 16 May 2022

HAL is a multi-disciplinary open access archive for the deposit and dissemination of scientific research documents, whether they are published or not. The documents may come from teaching and research institutions in France or abroad, or from public or private research centers.

L'archive ouverte pluridisciplinaire **HAL**, est destinée au dépôt et à la diffusion de documents scientifiques de niveau recherche, publiés ou non, émanant des établissements d'enseignement et de recherche français ou étrangers, des laboratoires publics ou privés.

Distributed under a Creative Commons Attribution - NonCommercial 4.0 International License

Showcasing research from the research teams of Dr N. Hoffmann, Prof. G. Lemercier (CNRS, Université de Reims Champagne-Ardenne, Reims, France) and Prof. A. Pedone (Università di Modena e Reggio Emilia, Modena, Italy). The image was created with the help of Jo-han Cruellas.

Synthesis and characterization of polymethine dyes carrying thiobarbituric and carboxylic acid moieties

A polymethine dye is formed by depolymerisation of pectin followed by chemical treatment with thiobarbituric acid. This transformation is used for the photometric detection of the pectin lyase activity. An efficient chemical synthesis of such compounds has now been developed which makes them available on larger scale. Furfural, a platform chemical from biomass, is used as starting compound. The resulting dyes have been characterized by spectroscopic and computational methods. The polymethine dye is a mono anion which is formed by deprotonation of a thiobarbituric acid moiety.

As featured in:

See Norbert Hoffmann *et al.*, *New J. Chem.*, 2022, **46**, 8971.

ROYAL SOCIETY OF CHEMISTRY

rsc.li/njc

Registered charity number: 207890

Synthesis and characterization of polymethine dyes carrying thiobarbituric and a carboxylic acid moieties †

Arthur Desvals[1], Mariagrazia Fortino[2], Corentin Lefebvre[1], Johann Rogier[1], Clément Michelin[1,3], Samy Alioui[1], Elodie Rousset[1], Alfonso Pedone[2], Gilles Lemercier[1], Norbert Hoffmann*[1]

[1] CNRS, Université de Reims Champagne-Ardenne, ICMR, Equipe de Photochimie, UFR Sciences, B.P. 1039, 51687 Reims, France, Phone: + 33 3 26 91 33 10, e-mail: norbert.hoffmann@univ-reims.fr

[2] Università di Modena e Reggio Emilia, via Campi 103, 41125 Modena, Italy

[3] Université Clermont Auvergne, CNRS, Clermont Auvergne INP, ICCF, 63000 Clermont-Ferrand, France

Abstract

An efficient synthesis of polymethine dyes carrying thiobarbituric and a carboxylic acid moiety has been developed. Such compounds play a key role in many photometric detections and quantifications of enzyme activities. In such tests, the metabolite of the enzyme activities is transformed into a β-dicarbonyl derivative. In the present study, this compound was prepared from furfural through organic synthesis. Its *in situ* transformation with thiobarbituric acid derivatives yields the target compounds on a gram-scale (0.4 to 0.6 g). A combined experimental and theoretical study of the photophysical properties of the synthesized compounds was carried out. Absorption and emission spectroscopy measurements highlighted a slight solvatochromism effect. The luminescence was quenched by molecular oxygen, indicating the partial triplet multiplicity character of the lowest excited state. Density Functional Theory (DFT) calculations have been applied for the evaluation of favoured conformations for these new compounds and the study of their optical properties. Within the Franck Condon principle, vibrationally resolved electronic one-photon absorption spectrum has been simulated. This simulation shows the presence of a major band followed by a vibronic sideband, typical of organic chromophores in solution. The performed computational study revealed that the transition from the ground to the first excited electronic state has a π-π^* character. Finally, TD-DFT energy level diagram calculations highlighted the presence of triplet states very close to the first singlet excited one, suggesting probable access to the triplet-excited state.

† Electronic supplementary information (ESI) available:

INTRODUCTION

The chromophoric system of polymethine dyes contains linear arrangements of π-conjugated bonds with an odd number of sp^2 hybridized carbon atoms.[1] The chains are flanked with electron donor or acceptor groups, often heterocycles. Either the polyene chain is substituted with the same group or it carries two different electron active groups. In the latter case, push-pull compounds[2] can be obtained. Polymethine dyes have been applied in many domains,[3] for example as sensors[4] or for photopolymerisation.[5] They interact with many biomacromolecules.[6] Most frequently, polymethine dyes are obtained by condensation of unsaturated C-H acidic compounds with unsaturated aldehydes thus generating a more or less extended π-conjugated sp^2-hybridized carbon chain[1,2,7] similar to those of carotenes. Most frequently, amines are used as auxochromic groups. The resulting subfamily of polymethine dyes is called cyanines (Figure 1).[1] They possess an enamine and an iminium function. The positive charge is delocalized over the polymethine core chain. Less frequently, polymethine dyes possessing a negative charge at the lateral auxochromic groups have been reported. They are called oxonols and the negative charge is delocalized over the polymethine chain. In this case, often barbituric acid derivatives are used. It is interesting to note that despite the different lateral functionalities the spectroscopic properties are very similar for compounds of both families possessing the same polymethine chain length.[8] Some commercial oxonols are used, for example, to assess the membrane potential of living cells.[9]

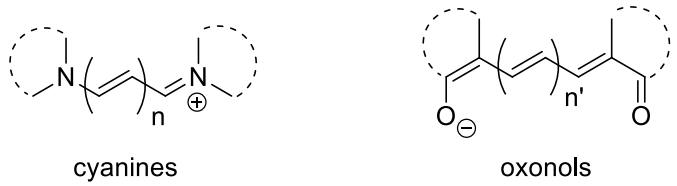

Figure 1. Two subfamilies of polymethine dyes: cyanines and oxonols.

Oxonols are attracting huge interest since they are formed from metabolites by condensation with thiobarbituric acid.[10] Therefore, the formation of these dyes indicates specific enzymatic activities,[11] as in the case of a pectin lyase activity summarized in Scheme 1.[12,13] Pectins are mainly composed of polygalacturonates. Their depolymerisation plays an important role in fruit juice processing or wine making since the viscosity is reduced and processes such as filtration, extraction of clarification is thus facilitated. Mainly two kinds of pectolytic activities exists: (1) Polygalacturonase in combination with pectin esterase and (2) pectinlyase.[12,14] In the first case galacturonic acid monomers are formed and in the second case the α,β-unsaturated uronic esters are formed which are transformed into the yellow formyl pyruvic acid derivative **4** (λ_{max} = 419 nm). Photometric tests developed on this basis are sensitive. However, the direct detection and quantification of **4** is rather unspecific since several other compounds also absorb in this spectral domain.[12] The selective transformation of **4** into a dye absorbing at longer wavelength was therefore performed. Thiobarbituric acid or its derivatives revealed to be particularly efficient since they lead almost quantitatively to the polymethine dyes which absorb at $\lambda_{max} \approx 550$ nm). Thus under the biochemical test conditions a polyene chain is formed that carries two identic auxochromic substituents at the ends and a carboxylic acid function. The above-mentioned activities are often concomitantly observed in enzyme preparations or microorganisms. Earlier studies revealed that this technique was not specific since also smaller amounts of galacturonic acid may be transformed into **4** and thus into the polymethine dyes.[15] The test conditions were optimised so that the selective detection of a pectin lyase activity became possible by this method.[12] This test is now most frequently

applied for the detection of a pectin lyase activity. However, the formation of cyanine dyes for this purpose should be less efficient since under the test conditions, they are less stable. Due to the presence of iminium function, these compounds undergo nucleophilic intermolecular or intramolecular addition by the carboxylic function.[16] Thus, the dye is decomposed. Due to the presence of three different acid functions in the dye – one carboxylic acid and two thiobarbituric acids-, it is important that deprotonation occurs at a thiobarbituric acid moiety in order to preserve the typical absorption properties of the oxonol polymethine dyes.

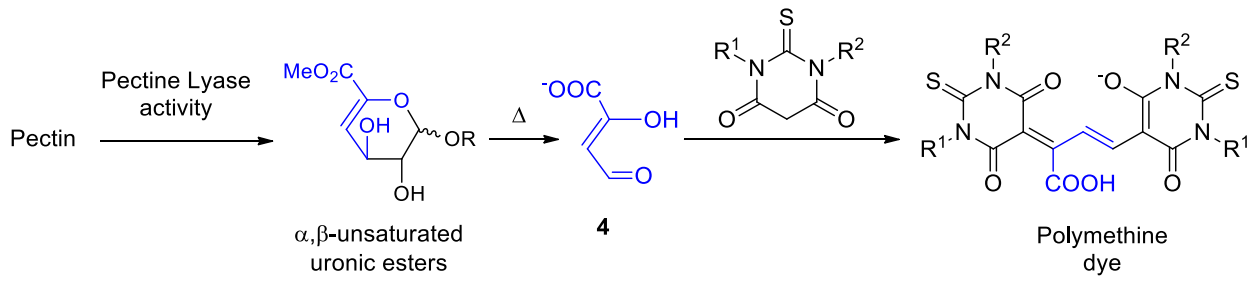

Scheme 1. Formation of a polymethine dye from the metabolite of the pectin lyase activity.

We became also interested in such dyes due to their potential physicochemical properties and further applications, for example in the fields of enzymology [10], radical polymerization as photoimitator [5,17] or as stimuli-responsive luminescent dyes. Therefore, the aim of this work was to devise a convenient chemical synthesis of such compounds in order to make them easily available on large scale and to determine various photophysical properties such as solvatochromism and acidity. To the best of our knowledge, only one of these compounds has been synthesized until now.[18] Ethyl ethoxymethylene pyruvate has been used as precursor of the chromophore or the core structure.

RESULTS AND DISCUSSION

Synthesis

5-Ethoxy-2[5H]-furanone **1** was used as starting material. This compound is easily available by photooxygenation of furfural and consecutive acetalization with ethanol.[19,20] In order to increase the oxidation state in the α position of the carboxylic function, α bromination was carried out (**2**) (Scheme 2).[21,22] In this step, addition of bromine takes place. Subsequent addition of triethylamine to the reaction mixture yields the desired compound **2**. Hydrolysis under basic conditions yields the formylpyruvate **4'** that is in tautomeric equilibrium with **4**. The tautomer **4'** is a derivative of malondialdehyde, which generates the core structure of many tri and pentamethine dyes. The anion is yellow (λ_{max} = 419 nm).[12] The condensation with thiobarbituric acid derivatives **3a,b** was carried out under acidic conditions. The final products **5a,b** were isolated as mono potassium salts.

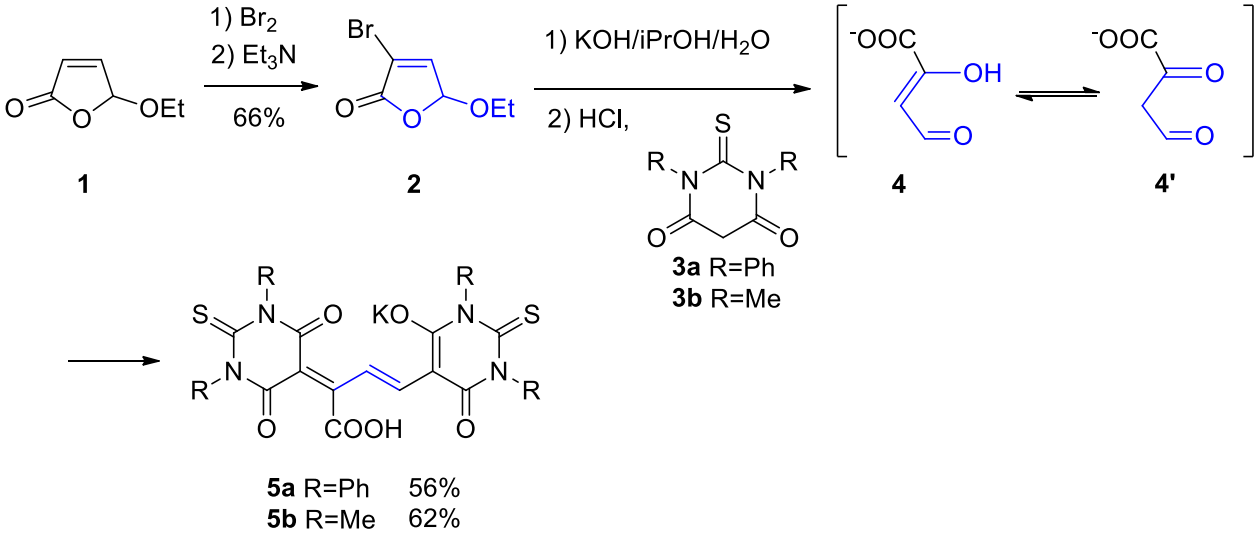

Scheme 2. Synthesis of two trimethine dyes carrying a carboxylic group.

Photophysical investigations

The electronic absorption spectra of compounds **5a** and **5b** in acetonitrile are very similar (see Figure S1 in the ESI). As illustrated in Figure 2 for compound **5a**, the UV-vis spectra in acetonitrile show a quite narrow absorption band centred around 554 nm (ε = 8.8 × 10^4 L·mol^{-1}·cm^{-1}) and 551 nm (ε = 8.1 × 10^4 L·mol^{-1}·cm^{-1}) for compound **5a** and **5b**, respectively, with a hypsochromic shoulder at around 515 nm typical for such dyes.[23,24] In agreement with calculations performed in this study (*see computational studies below*), and most of the literature[25], the shoulder arises from the coupling of vibrations of the polymethine chains with the S_0-S_1 electronic transition. This is the most probable attribution even if in the literature sometimes, these two absorption bands are assigned to S_0-S_1 and the more energetic S_0-S_2 electronic transitions.[26] The vertical absorption is dominated by the HOMO - LUMO transition and corresponds to a π– π * transition, which governs the optical properties of similar dyes.[27,28] (*see computational studies below*). This localized character of the involved electronic transitions is in good agreement with the observed low solvatochromism observed in absorption for these two compounds with shifts of only 100 cm^{-1} for compound **5a** (Figure S2 and S4), and 160 cm^{-1} for compound **5b** (Figure S3), from dichloromethane to DMSO and acetonitrile to DMSO, respectively. It has to be mentioned that less solvents could be used for chromophore **5b** due to solubility issues in less dipolar solvents (so it was not possible to use dichloromethane). For protic solvents (water and methanol, which gave similar results) a small blue shift was observed compared to aprotic solvents, from 554 nm to 548 nm for example (200 cm^{-1}, see Figure S3), for **5a** and from DMSO to water.

After excitation at 545 nm, the emission is centred at 575 nm and 564 nm in acetonitrile (568 and 566 nm in THF) for **5a** and **5b**, respectively (see Figure 2 and Fig. S5, respectively). The excitation spectrum fits quite well with the absorption spectrum for **5a** and **5b**. For both compounds, the low Stokes shift value (450 cm^{-1} and 225 cm^{-1} in acetonitrile for example, for compound **5a** and **5b**, respectively) indicates that a moderate geometry change occurs from the lowest in energy Franck-Condon excited state (S_0-S_1 electronic transition) to the emissive excited state.

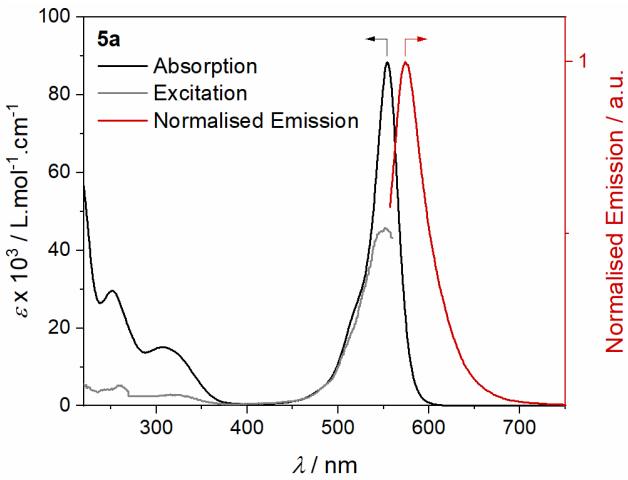

Figure 2: Absorption (black), excitation spectrum (grey) and emission (red) spectra of compound **5a** in acetonitrile (conc. 6.1×10^{-6} mol·L^{-1})

This small Stokes shift and the related large overlap between the absorption and emission spectra can partially explain the low emission quantum yield (lower than 1% in water and acetonitrile, evaluated using quinine sulphate as reference). The solvatochromic effect on the emission spectra of compound **5a** was investigated as depicted in Figure 3 (See Figure S5 for compound **5b**). As the emission band is not largely affected by the nature of the (protic and aprotic) solvents, and more particularly their dipolar moment, this confirms that the absorption can be mainly attributed to a π-π* transition related to the HOMO – LUMO gap (see calculations paragraph). Nevertheless, the small hypsochromic shift observed (around 330 cm^{-1} for compound **5a** with λ_{max} emission equal to 579 nm and 568 nm in dichloromethane and DMSO, respectively and concerning aprotic solvents used), is in good agreement with a decrease of the dipolar moment going from the fundamental state to the emissive excited-state and may confirm the charged character of the fundamental state. The results obtained with recording the emission intensity (around 560 nm) in the presence of different amounts of soluble oxygen showed that compound **5b** can act as photosensitizer (PS) since its emissive excited-state is sensitive to the presence of ground state dioxygen (see Figure S6). Since (triplet) ground state oxygen is an efficient dynamic or collisional quencher of triplet excited states, Stern-Volmer analysis can provide a measure of the efficiency of this quenching process in terms of the quenching constant K_{sv}.

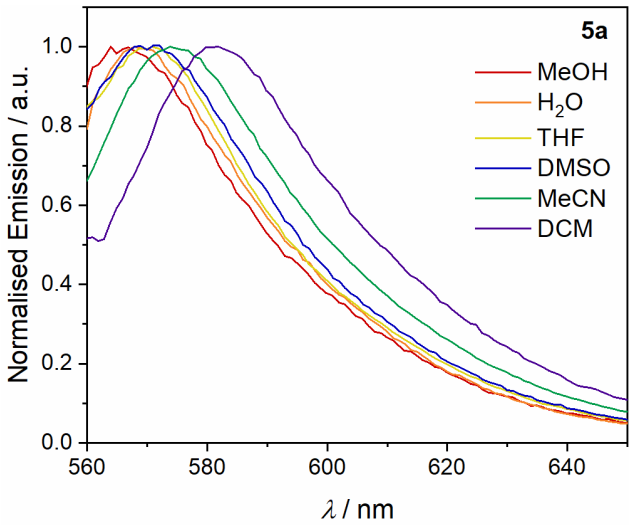

Figure 3: Emission spectra of compound **5a** in several solvents.

The dependence of emission intensity with quencher concentration ($^3O_2$), is given by the following equation:

$I_0/I = 1 + K_{SV}[O_2] = 1 + k_q \tau_0 [O_2] = 1 + k_q \tau_0 K_{Hsolv} P_{O2}$ (1)

I_s are emission intensities, K_{SV} is the Stern-Volmer quenching constant, k_q is the bimolecular rate constant for quenching of the excited state, and K_H is the Henry constant of O_2 (gas) in a given solvent. The subscript « 0 » denotes the values of the quantity in the absence of the quencher. Plots of I_0/I *vs* oxygen concentration will be linear with slope equal to K_{SV} if there is a single class of luminophore that are all equally accessible to the quencher. In this regard, the potential of **5b** to act as a triplet oxygen sensitizer was assessed by determining the emission intensity in degassed, air equilibrated and oxygen-saturated acetonitrile solutions following excitation into the low energy absorption bands at 530 nm excitation in DMSO (see Figure 4). With a solubility of dioxygen of around 2.4 mmol/L in DMSO[29], the K_{SV} quenching constant can be estimated to 30 M^{-1}, which is quite compatible with potential applications (see for example ref 30).

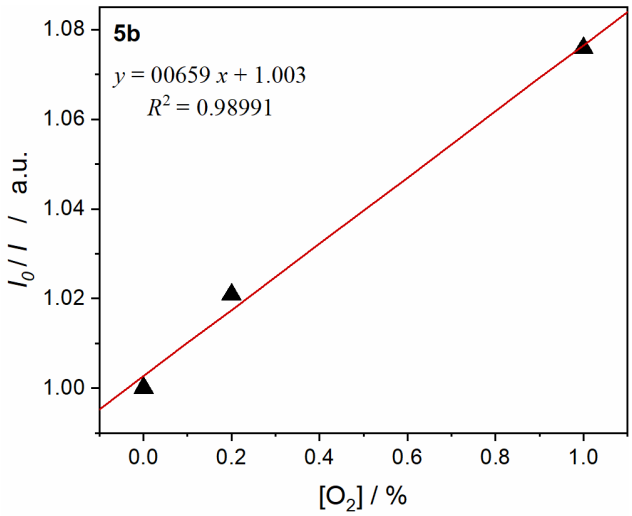

Figure 4: Stern-Volmer plot for compound **5b** in DMSO. Experimental points in black triangles and best fit in red.

The same study performed with compound **5a** (carrying four N-Ph groups, under the same conditions of temperature and solvent), showed no influence of ground state $^3O_2$ on the emission properties (see Figure S7). This is in agreement with a probably lower triplet character of its emissive excited state.

Computational studies

Three possible tautomeric structures for **5b** polymethine dye, considered mainly favoured for their significant mesomeric effect and for the presence of stabilizing hydrogen bonds, have been theoretically investigated at density functional theory (DFT) level, see Scheme 3.

Tautomer **A** presents a deprotonated function on the carboxylic moiety linked to the C=C chain, while both **B** and **C,** have a deprotonated function on the thiobarbituric moiety but differ by the orientation of the carboxylic function on the C=C chain. Thus, **B** and **C** are conformers.

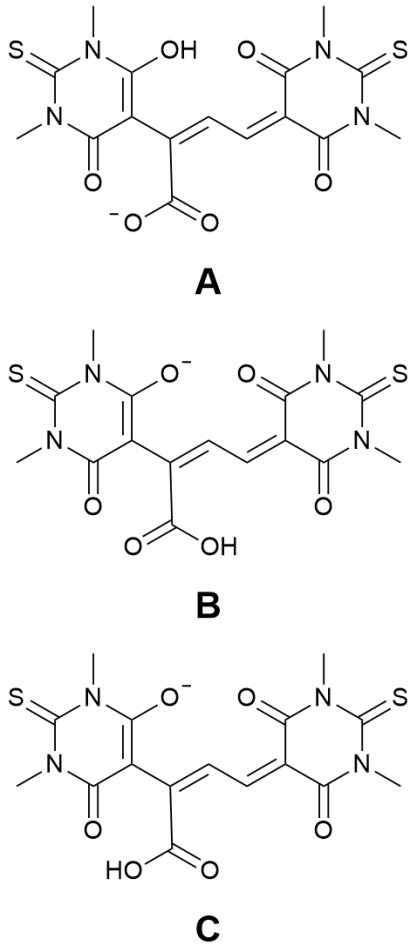

Scheme 3. A representation of the three investigated tautomeric structures for **5b** compound.

In Figure 5, the optimized structures for tautomers **A** and **B** / **C**, calculated at B3LYP-D3/6-31+G(d,p) level of theory and taking into account acetonitrile solvent effects by using implicit solvation model, are reported (see Supporting Information for the optimized Cartesian coordinates of the tautomer structures). For tautomer **A**, a hydrogen bond between the alcoholic function and the carbonyl group belonging to the two rings has been computed with a distance of 2.05 Å, whereas for tautomer **C** a hydrogen bond with a distance of 1.46 Å has been calculated between the carboxylic function on the C=C chain and the carbonyl group on the ring.

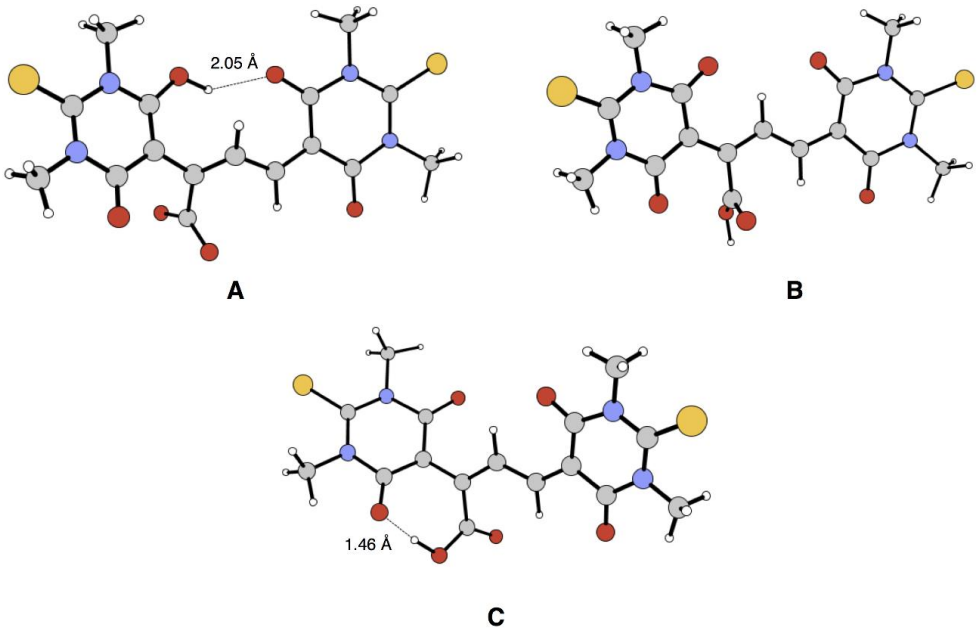

Figure 5. Optimized structures for tautomers **A** and **B** / **C**, calculated at B3LYP-D3/6-31+G(d,p) level of theory. Main computed hydrogen bond distances are also reported.

The computed energy values and the obtained stability order highlighted in Table 1 show that the structure **B** is the more stable one, followed by **C** with an energy difference of 2.20 kcal/mol. In agreement with experimental observation, this result indicates that deprotonation on thiobarbituric moiety is preferred. Deprotonation of the carboxylic acid function is less favourable. For example, UV spectra of our compounds **5a** and **5b** are almost identical to those obtained from thiobarbituric methine compounds, which do not carry a carboxylic function.[11,31]

Table 1. Energy values for the investigated tautomers, computed at B3LYP-D3/6-31+G(d,p) level of theory.

Tautomer	***E* (Hartree)**	**Relative energy (kcal/mol)**
A	-2085.560229	17.62
B	-2085.588303	0
C	-2085.584790	2.20

Starting from these first computational results, further deeper theoretical investigations have been performed on the more favoured tautomer **B**, in order to better analyse its optical properties and, specifically, the features of the transition from the ground state S_0 to the first excited one S_1, having the highest oscillator strength value (see Supporting Information for the oscillator strength values computed for the first three singlet excited states). In Figure 6, the vibrationally resolved electronic (vibronic) one-photon absorption spectrum simulated for tautomer **B** is reported. The vibronic spectrum has been computed within the Franck-Condon principle, at TI VG|FC level of theory (see Computational Details), neglecting temperature effects and implicitly taking into account for the acetonitrile solvent effects. The energy for the transition 0-0 has been predicted to be 18693 cm^{-1} (~534 nm). The simulated absorption

spectrum presents the typical shape found for organic chromophores in solution with a main peak located at around 530 nm and a minor peak, representing a vibronic sideband, located at 500 nm.

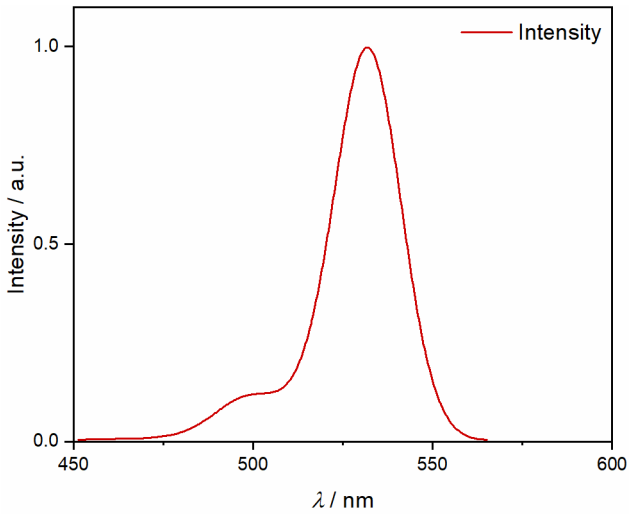

Figure 6. Simulated vibrationally resolved absorption spectrum for tautomer **B**, calculated at TI VG|FC level and using B3LYP-D3 as density functional and 6-31+G(d,p) as basis set. The acetonitrile solvent effects have been taken into account by using PCM implicit solvation method. A Gaussian distribution of 350 cm^{-1} has been used to simulate the broadening.

For a deeper study of the nature of the electronic transition, we performed a Quantum Mechanical (QM) analysis of the frontier molecular orbitals. This study reveals that the S_0-S_1 transition involves the highest occupied molecular orbital (HOMO) and the lowest unoccupied molecular orbital (LUMO), shown in Figure 7 (see Figure S7 and S8 of Supporting information for computed HOMOs and LUMOs of tautomers **A** and **C**). The HOMO and LUMO are mainly delocalized on the rings and along the C=C chain, showing the π-π^* character of the transition in agreement with the experimental finding**.**

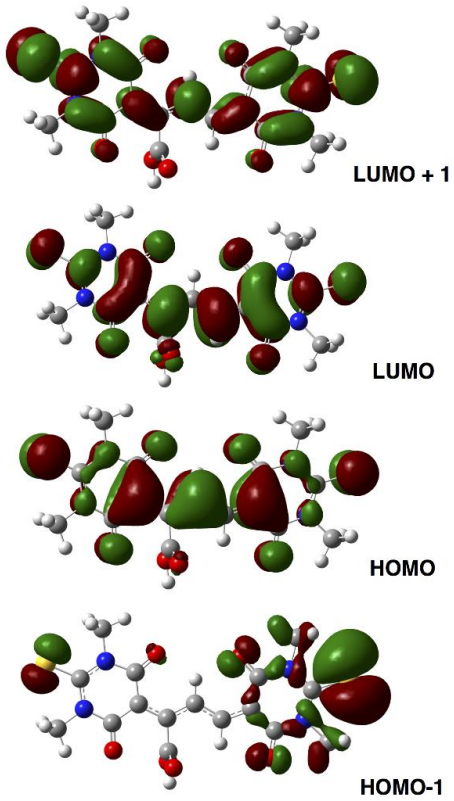

Figure 7. Frontiers molecular orbitals (HOMO-1, HOMO, LUMO, and LUMO+1) computed for tautomer **B** at B3LYP-D3/6-31+G(d,p) level of theory.

Finally, as last step of the theoretical investigation, the energy level diagram has been computed at B3LYP-D3/6-31+G(d,p) level of theory and reported in Figure 8. The performed energy level diagram analysis highlights the presence of a triplet state (T_4) located at 2.568 eV, very close to first singlet excited state (S_1), and located at 2.579 eV, with an energy difference of 0.011 eV. This finding may suggest a possible access to the triplet electronic excited state.

It is worth emphasizing that, slight discrepancies found in terms of energy level positions and experimental band position are due to the fact that vertical excitation energy can be intrinsically overestimated by TD-DFT method with respect to the experiments or high-level post-HF calculations. Indeed, TD-DFT accuracy is strongly dependent on the nature of the considered state, the used functional and a proper account of vibrational structure.[32]

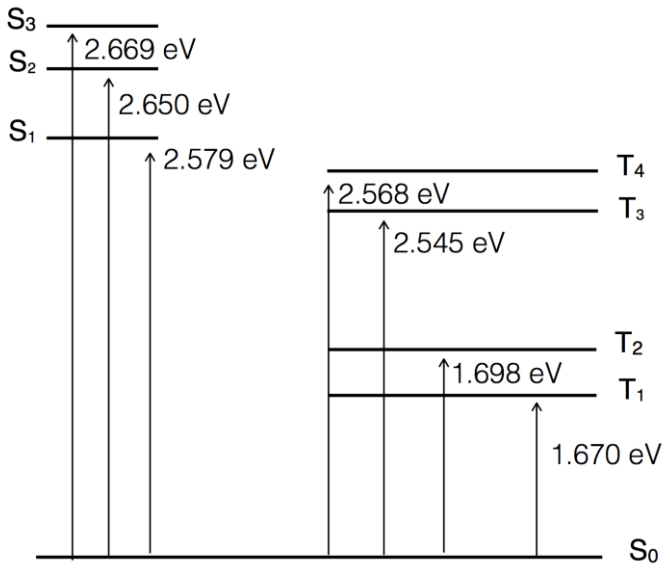

Figure 8. Energy level diagram computed at B3LYP-D3/6-31+G(d,p) level of theory for tautomer **B**.

CONCLUSIONS

Trimethine dyes carrying a carboxylic function are formed by condensation of thiobarbituric acid derivatives with formylpyruvate, a consecutive product of a metabolite of several enzymatic activities such as pectin lyase. We have developed a convenient organic synthesis to prepare such compounds. The electronic excitation results from a π-π* transition with a low solvatochromism. The low Stokes shift indicates rigid structures during the electronic transitions. The emission occurs from an excited state with a triplet state character. The corresponding intersystem crossing from the S_1 state to the triplet-excited state is favoured by the presence of the thiocarbonyl function. The trimethine dyes are acidic and the deprotonation occurs at the thiobarbituric moieties while deprotonation of the carboxylic function is unfavourable. This is important to preserve the typical absorption properties of the anionic oxonol polymethin dye. Therefore, the absorption spectra are very similar to those of related thiobarbituric trimethine dyes without a carboxylic function.

EXPERIMENTAL

General. NMR spectra were recorded on Bruker spectrometers operating at 500 MHz for ^{1}H and 126 MHz for ^{13}C. For ^{1}H NMR spectra, chemical shifts are reported in parts per million (ppm) with reference to residual protonated solvent (δ = 7.26 ppm for $CHCl_3$, δ = 2.50 ppm for DMSO-d_6) as internal standard. For ^{13}C NMR spectra, chemical shifts are reported in parts per million (ppm) with reference to the deuterated solvent (δ = 77.16 ppm for $CDCl_3$, δ = 39.52 ppm for DMSO-d_6) as an internal standard. Splitting patterns for ^{1}H signals are designated as s (singlet), d (doublet), t (triplet), q (quartet), m (multiplet) or br. (broad), and coupling constants (J) are reported in Hz. UV/Vis and emission spectra were recorded on a Cary 5000 UV-2401PC spectrophotometer and a Varian Cary Eclipse spectrofluorometer, respectively. Infrared (IR) spectra were recorded for solid samples on a Nicolet AVATAR 320 FT-IR, maximum absorbances (ν) are given in cm^{-1}. High-resolution mass spectrometry (HR-

MS) data were recorded using a spectrometer equipped with an electrospray ionisation source (ESI-MS) in positive mode associated with a TOF analyzer. Elemental analyses were performed with a Flash EA 1112 Series Thermo Electron analyzer at 950 °C. Inductively coupled plasma mass spectrometry (ICP-MS) measurements were recorded with a Thermo Scientific iCAP 6000 Series ICP Emission Spectrometer using a potassium standard. Photochemical reactions were performed using a medium pressure mercury vapor lamp set to 400 W immerged in a 2 L quartz reactor. N,N'-dimethylthiourea (99 %), N,N'-diphenylthiourea (98 %) and Furfural (98 %) were purchased from Merck. N,N'-dimethylthiobarbituric acid,[33] N,N'-diphenylthiobarbituric acid,[34] 5-Hydroxyfuran-2(5H)-one and Ethoxyfuranone were prepared according to the literature, and their spectroscopic data are in agreement with those previously reported. Organic extracts were dried over magnesium sulfate (VWR Chemicals, 98%) before evaporation under reduced pressure. Flash chromatography was performed on silica gel columns (40–63 μm). Analytical thin-layer chromatography was carried out with Kieselgel 60F254 plates from Merck.

3-bromo-5-ethoxyfuran-2(5H)-one (**2**). In a two-necks round bottom flask was added Ethoxyfuranone (3.06 g, 24 mmol, 1.0 eq.) and CH_2Cl_2 (20 mL). The mixture was vigorously stirred and Br_2 (3.8 g, 24 mmol, 1.0 eq.) was added dropwise at room temperature. When the solution took a yellow color, triethylamine (4 mL, 29 mmol, 1.2 eq.) was added. The mixture was stirred during 18 h at room temperature. The solution was poured into a separatory funnel. The organic layer was washed with H_2O, brine, dried over $MgSO_4$, filtrated, and concentrated under reduced pressure. The residue was purified by column chromatography (petroleum ether/diethylether = 9:1) to afford compound **2** as a clear liquid (3.9 g, 66 %). R_f = 0.32 (petroleum ether/diethylether = 9:1, $KMnO_4$ revelator). Spectroscopic data are in agreement with those previously reported. [19,21] ^{1}H NMR (500 MHz, $CDCl_3$, ppm): δ 7.27 (d, *J* = 1.4 Hz, 1H; CH), 5.87 (d, *J* = 1.4 Hz, 1H; CH), 3.94 (dq, *J* = 11.9 Hz, *J* = 7 Hz, 1H; CH_2), 3.77 (dq, *J* = 11.9 Hz, *J* = 7.1 Hz, 1H; CH_2), 1.28 (dd, *J* = 7.1 Hz, *J* = 7 Hz, 3H; CH_3). $^{13}C\{^1H\}$ NMR (126 MHz, $CDCl_3$, ppm): δ 166.2 (Cq), 147.1 (CH), 118.3 (Cq), 102.5 (CH), 66.4 (CH_2), 15.1 (CH_3).

Compound **5a**. In a round bottom flask was added 3-bromo-5-ethoxyfuran-2(5H)-one (414 mg, 2 mmol, 1.0 eq.) and isopropanol (20 mL). The solution was stirred at reflux and KOH (2.4 mL of a 1 M solution, 2.4 mmol, 1.2 eq.) was added. The solution turned yellow/orange, after 5 min. HCl (2.8 mL of a 1M solution, 2.8 mmol, 1.4 eq.) was added. After the addition, the solution lost the yellow color. N,N'-diphenylthiobarbituric acid (890 mg, 3 mmol, 1.5 eq.) was added and the solution immediately turned to a strong purple colour. The mixture was cooled to room temperature and was stirred during 3 h. The solvent was removed in vacuo and the residue was directly adsorbed onto silica to be purified by column chromatography (ethyl acetate to ethyl acetate/MeOH = 9:1 to 8:2) to yield compound **5a** as a purple powder (562 mg, 56 %). ^{1}H NMR (500 MHz, DMSO-d_6, ppm): δ 9.11 (d, *J* = 14.7 Hz, 1H; =CH), 8.05 (d, *J* = 14.7 Hz, 1H; =CH), 7.40-7.63 (m, 8H; Ar-H), 7.33-7.29 (m, 4H; Ar-H), 7.23-7.18 (m, 8H; Ar-H). $^{13}C\{^1H\}$ NMR (126 MHz, DMSO-d_6, ppm): δ 179.8 (C=S), 178.9 (C=S), 169.0 (COOH), 161.9 (=C-OH or C=O), 160.4 (2 C=O or =C-OH), 159.9 (C=O or =C-OH), 154.4 (=CH), 141.0 (Ar-Cq), 140.9, (Ar-Cq), 140.7 (Ar-Cq), 129.3 (Ar-CH), 128.6 (Ar-CH), 127.4 (Ar-CH), 114.6 (=CH), 103.7 (Cq), 97.6 (Cq). IR: ν (cm^{-1}) 3559, 3432, 3204, 1641, 1537, 1488, 1354, 1306, 1195, 1152. HRMS (ESI): *m/z* $[M+H]^+$ calcd for $[C_{36}H_{25}N_4O_6S_2]^+$, 673.1215; found, 673.1216. Elemental analysis: calcd for $[C_{36}H_{23}N_4O_6S_2K]\ \frac{7}{2}\ H_2O$: N, 7.13; C, 55.92; H, 3.90; S, 7.84; found: N, 7.24; C, 55.87; H, 3.91; S, 8.29. ICP-MS (K emission at 766 nm): calcd for a $1x10^{-4}$mol/L solution of **5a** in nitric acid diluted in water; concentration of K found: $2.98x10^{-6}$mol/L (the sample could not be solubilized entirely thus the analysis is qualitative).

Compound **5b**. In a round bottom flask was added 3-bromo-5-ethoxyfuran-2(5H)-one (406 mg, 1.96 mmol, 1.0 eq.) and isopropanol (5.1 mL). The solution was stirred at reflux and KOH (2.35 mL of a 1 M solution, 2.35 mmol, 1.2 eq.) was added. The solution turned yellow/orange, after 5 min HCl (2.75 mL of a 1M solution, 2.75 mmol, 1.4 eq.) was added. After the addition, the solution lost the yellow color. N,N'-dimethylthiobarbituric acid (608 mg, 3.53 mmol, 1.8 eq.) was added and the solution immediately turned to a strong purple colour. The mixture was cooled to room temperature and was stirred during 3 h. The mixture was filtrated and washed using CH_2Cl_2. The powder was put into a round bottom flask and CH_2Cl_2 (10 ml) was added, the mixture is stirred at reflux for 30 min. The mixture was filtrated and dried to yield compound **5b** (467 mg, 62 %) as a purple powder. ^{1}H NMR (500 MHz, DMSO-d_6, ppm): δ 9.27 (d, J = 14.7 Hz, 1H; =CH), 8.10 (d, J = 14.7 Hz, 1H; =CH), 3.6 (s, 12H; CH_3). ^{13}C{^{1}H} NMR (126 MHz, DMSO-d_6, ppm): δ 178.8 (C=S), 177.9 (C=S), 169.2 (COOH), 162.1 (=COH or =C=O), 161.5 (C=O or =COH), 160.0 (C=O or =COH), 159.7 (C=O or =COH), 155.1 (=CH), 115.2 (=CH), 103.2 (Cq), 97.1 (Cq), 35.2 (CH_3), 35.4 ($2CH_3$), 35.0 (CH_3). IR: ν (cm^{-1}) 3428, 3399, 3376, 2946, 1743, 1634, 1588, 1549, 1497, 1463, 1428, 1407, 1355, 1330, 1230, 1192, 1168, 1117, 1078. HRMS (ESI) *m/z* $[M+H]^+$ calcd for $[C_{16}H_{17}N_4O_6S_2]^+$, 425.0590; found, 425.0590. Elemental analysis: calcd for $[C_{16}H_{15}N_4O_6S_2K]$ ½ H_2O: N, 11.88; C, 40.75; H, 3.42; S, 13.60; found: N, 11.79; C, 41.00; H, 3.44; S, 13.37. ICP-MS (K emission at 766 nm): calcd for a 1.3x10^{-4}mol/L solution of **5b** in nitric acid diluted in water; concentration of K found: 1.34x10^{-4}mol/L.

COMPUTATIONAL DETAILS

All computations have been performed at Density Functional Theory (DFT) level of theory, and its time dependent extension (TD-DFT), by using Gaussian09 suite of quantum chemical program.[35] The Becke's three-parameter hybrid functional (B3) with the Lee, Yang, and Parr (LYP) expression for the nonlocal correlation, B3LYP,[36] has been used, since it accurately describes organic molecule electronic structures and energetic properties.[37] The dispersion energy contributions have been included through the procedure proposed by Grimme,[38] with the so-called D3 set of parameters. In all computations, 6-31+G(d,p) has been used as basis set for all atoms. The effect of acetonitrile as solvent has been taken into account by using the integral equation formalism for the polarizable continuum model (PCM).[39]

For the vibrationally resolved electronic one-photon absorption spectrum, the time independent framework (TI, which is a sum over states approach) has been used in conjunction with the Vertical Gradient (VG) approximation for the evaluation of the PES of the initial and final electronic states. Within the VG approximation, the PES of the initial state has been computed about its own minimum, whereas for the final state only the energy gradient has been computed by using the geometry of the initial state. This procedure has been chosen since no huge geometry modifications are expected during the electronic transition. Regarding the description of the electronic transition dipole moment, the Franck-Condon (FC) approximation has been used, assuming a constant dependence of the transition dipole moment on the nuclear coordinates. In the text, TI VG|FC refer to the used procedure for the vibronic simulation. A more extensive presentation of the computational strategies available for the simulation of vibronic spectra can be found in ref 40.

CONFLICTS OF INTEREST

There are no conflicts to declare.

ACKNOWLEDGMENTS

We thank Lucas Fortier for help with synthetic work. This research studies were supported by the Agence Nationale de Recherche (ANR, Project PICPOSS), the Communauté Urbaine du Grand Reims and the Université de Reims Champagne-Ardenne. A. P. and M. F. thank high performance computer facilities of Università di Modena and Reggio Emilia.

REFERENCES

[1] H. Zollinger, *Color Chemistry*. Verlag Helvetica Chimica Acta, Zürich, 2003.
[2] M. Klikar, V. Jelínková, Z. Růžičková, T. Mikysek, O. Pytela, M. Ludwig and F. Bureš, Malonic Acid Derivatives on Duty as Electron-Withdrawing Units in Push-Pull Molecules. *Eur. J. Org. Chem.* 2017, **2017**, 2764-2779. K. C. Kreß, T. Fischer, J. Stumpe, W. Frey, M. Raith, O. Beiraghi, S. H. Eichhorn, S. Tussetschläger and S. Laschat, Influence of Chromophore Lengh and Acceptor Groups on the Optical Properies of Rigidified Merocyanine Dyes. *ChemPlusChem* 2014, **79**, 223-232.
[3] A. Mishra, R. K. Behera, P. K. Behera, B. K. Mishra and G. B. Behera, Cyanines during the 1990s: A Review. *Chem. Rev.* 2000, **100**, 1973-2011.
[4] W. Sun, S. Guo, C. Hu, J. Fan and X. Peng, Recent Development of Chemosensors Based on Cyanine Platforms. *Chem. Rev.* 2016, **116**, 7768-7817. B. Li, M. Zhao and F. Zhang, Rational Designing of Near-Infrared-II Organic Molecular Dyes for Bioimaging and Biosensing. *ACS Materials Lett.* 2020, **2**, 905-917. J. M. Hales, S. Barlow, H. Kim, S. Mukhopadhyay, J.-L. Brédas, J. W. Perry and S. R. Marder, Design of Organic Chromophores for All-Optical Signal Processing Applications. *Chem. Mater.* 2014, **26**, 549-560. J. L. Bricks, A. D. Kachkovskii, Y. L. Slominskii, A. O. Gerasov and S. V. Popov, Molecular design of near infrared polymethin dyes: A review. *Dyes Pigm.* 2015, **121**, 238-255. J. Pączkowski, J. Kabatc and B. Jędrzejewska, Polymethine Dyes as Fluorescent Probes and Visible-Light Photoinitiators. *Top. Heterocycl. Chem.* 2008, **14**, 183-220.
[5] B. Strehmel, T. Brömme, C. Schmitz, K. Reiner, S. Ernst and D. Keil, NIR-Dyes for Photopolymers and Laser Drying in Graphic Industry, In *Dyes and Chromophores in Polymer Science* (J. Lalevée, J.-P. Fouassier, Eds.) Wiley, London, 2015, pp. 213-249.
[6] A. S. Tatikolov, Polymethine dyes as spectral-fluorescent probes for biomacromolecules. *J. Phtochem. Photobiol. C* 2012, **13**, 55-90. H. Görner and A. K. Chibisov, Photoprocesses in Polymethine Dyes: Cyanines and Spiropyran Derived Merocyanines. In *CRC Handbook of Photochemistry and Photobiology, 2nd Ed.* (W. Horspool, F. Lenci, Eds.) CRC Press, Boca Raton, 2004, pp 36/1-36/21. A. V. Kulinich and A. A. Ishchenko, Merocyanine dyes: synthesis, structure, properties and applications. *Russ. Chem. Rev.* 2009, **78**, 141-164.
[7] M. Panigrahi, S. Dash, S. Patel and B. K. Mishra, Synthesis of cyanines: a review. *Tetrahedron* 2012, **68**, 781-805.
[8] For an example see: P. D. Ries and C. J. Eckhardt, Electronic Spectra and Structure of a Carbocyanine-Oxonol Mixted Cye Crystal. *J. Phys. Chem.* 1987, **91**, 5020-5026.
[9] R. W. Horobin, Polymethine dyes – 1. Cyanines, oxonols, benzimidazoles, indolenines and azamethines. In *Conn's Biological Strains, 10th Ed.* (R. W. Horobin, J. A. Kiernan, Eds.) Taylor & Francis, London, 2002 pp. 323-348. H. M. Shapiro, Membrane Potential Estimation by Flow Cytmetry. *Methods* 2000, **21**, 271-279. J. Plasek, K. Sigler, Slow fluorescent indicators of membrane potential: a survey of different approaches to probe response analysis. *J. Photochem. Photobiol. B* 1996, **33**, 101-124.
[10] F. M. Unger, The Chemistry and Biological Significance of 3-Deoxy-d-manno-2-Octulosonic Acid (KDO). *Adv. Carbohydr. Chem. Biochem.* 1981, **38**, 323-388.
[11] K. Nakashima, T. Ando, K. Nakamura and S. Akiyama, A convenient method for a sensitive colorimetric determination of lipoperoxides qith 1,2-diphenyl-2-thiobarbituric acid. *Chem. Pharm. Bull.* 1983, **31**, 2523-2525. H. Auterhoff and L. Jäger, Zur Kenntnis der Nachweisreaktionen der Sorbinsäure mit Thiobarbitursäure. *Arch. Parmaz.* 1974, **307**, 234-236. H. Schmidt, Über Thiobarbitursäure-Methin-Farbstoffe. *Fette Seifen Anstrichm.* 1959, **61**, 881-886. R. O. Sinnhuber, T. C. Yu and T. C. Yu, Characterization of the red pigment formed in the 2-thiobarbituric acid determination of oxidative rancidity. *J. Food Sci.* 1958, **23**, 626-634.

[12] M. Nedjma, N. Hoffmann and A. Belarbi, Selective and Sensitive Detection of Pectin Lyase Activity Using a Colorimetric Test: Application to the Screening of Microorganisms Possessing Pectin Lyase Activity. *Anal. Biochem.* 2001, **291**, 290-296.
[13] H. Neukom, Über Farbreaktionen von Uronsäuren mit Thiobarbitursäure. *Chimia* 1960, **14**, 165-167. P. Albersheim, H. Neukom and H. Deuel, Splitting of Pectin Chain Molecules in Neutral Solutions. *Arch. Biochem. Biophys*. 1960, **90**, 46-51. A. Weissbach and J. Hurwitz, The formation of 2-Keto-3-deoxyheptonic Acid in Extracts of Echerichia coli B. *J. Biol. Chem.* 1959, **234**, 705-709. A. P. Vesuna and A. S. Nerukar, Biocontrol impact of AHL degrading actinobacteria on quorum sensing regulated virulence of phytopathogen Pectobacterium carotovorum subsp. carotovorum BR1. *Plant Soil* 2020, **453**, 371-388. E. Tasgin, A. Babagil and H. Nadaroglu, Immobilization of Purified Pectin Lyase from Acinetobacter calcoaceticus onto Magnetic Carboxymethyl Cellulose Nanoparticles and Its Usability in Food Industry. *J. Chem.* 2020, **2020**, 4791408. V. S. Thite, A. S. Nerukar and N. N. Baxi, Optimization of concurrent production of xylanolytic and pectinolytic enzymes by Bacillus safensis M35 and Bacillus altitudinis J208 using agro-industrial biomass through Response Surface Methodology. *Sci Rep.*2020, **10**, 3824. P. Tehranchian, R. J. Adair, T. T. H. Van, P. D. Morrison, H. Williams and A. C. Lawrie, Biological Control of the Noxious Weed Angled Onion (Allium triquetrum) Thwarted by Endophytic Bacteria in Victoria, Australia. *Australas. Plant Pathol.* 2020, **49**, 373-392. P. Kohli, S. N. Sharma and R. Gupta, Statistical optimization of production conditions of alkaline pectin lyase from Bacillus cereus using response surface methodology. *Biocatal. Biotransform.* 2017, **35**, 417-426. F. Xu, F. Dong, P. Wang, H.-Y. Cao, C.-Y. Li, X.-H. Pang, Y.-Z. Zhang and X.-L. Chen, Novel Molecular Insights into the Catalytic Mechanism of Marine Bacterial Alginate Lyase AlyGC from Polysaccharide Lyase Family 6. *J. Biol. Chem.* 2017, **292**, 4457-4468. A. H. Badur, S. S. Jagtap, G. Yalamanchili, J.-K. Lee, H. Zhao and C. V. Rao, Alginate Lyases from Alginate-Degrading Vibrio splendidus 12B01 Are Endolytic. *Appl. Environ. Microbiol.* 2015, **81**, 1865-1873.
[14] G. S. N. Naidu and T. Panda, Production of pectolytic enzymes – a review. *Bioprocess Eng.* 1998, **19**, 355-361. P. Alimardani-Theuil, A. Gainvors-Claisse and F. Duchiron, Yeasts: An attractive source of pectinases – From gene expression to potential applications: A review. *Process Biochem.* 2011, **46**, 1525-1537. S. Samanta, Microbial Pectinases: A Review on Molecular and Biotechnological Prerspectives. *J. Microbiol. Biotech. Food Sci.* 2019, **9**, 248-266.
[15] R. M. Cooper and R. K. S. Wood, Regulation of synthesis of cell wall degrading enzymes by Veticillium albo-atrum and Fusarium oxysporum f. sp. Lycopersici. *Physiol. Plant Pathol.* 1975, **5**, 135-156.
[16] M. Henary and M. Mojzych, Stability and Reactivity of Polymethine Dyes in Solution. *Top. Heterocycl. Chem.* 2008, **14**, 221-238.
[17] J. Pączkowski, J. Kabatc and B. Jędrzejewska, Polymethine Dyes as Fluorescent Probes and Visible-Light Photoinitiators for Free Radical Polymerization. *Top. Heterocycl. Chem.* 2008, **14**, 183-220.
[18] R. Kuhn and P. Lutz, Über Formyl-brenztraubensäure und den Farbstoff der Warren Reaktion. *Biochem. Z.* 1963, **338**, 554-560.
[19] G. O. Schenck, Photochemische Reaktionen II Über die unsensibilisierte und photosensibilisierte Autoxidation von Furanen. *Justus Liebigs Ann. Chem.* 1956, **584**, 156-176. L. Cottier, G. Descotes, H. Nigay, J.-C. Parron and V. Grégoire, Photo-oxygénation des dérivés de l'hyddroxyméthyl-5 furfural-2. *Bull. Soc. Chim. Fr.* 1986, 844-850. I. L. Doerr and R. E. Willette, α,β-Unsaturated Lactones. I. Condensation of 5-Bromo-2(5H)-furanones with Adenine and Uracil Derivatives. *J. Org. Chem.* 1973, **38**, 3878-3887. S. Marincović, C. Brulé, N. Hoffmann, E. Prost, J.-M. Nuzillard and V. Bulach, Origin of Chiral Induction in Radical Reactions with the Diastereoisomers (5R)- and (5S)-5-l-Menthyloxyfuran-2(5H)-one. *J. Org. Chem.* 2004, **69**, 1646-1651. A. Gassama, C. Ernenwein, A. Youssef, M. Agach, E. Riguet, S. Marinković, B. Estrine and N. Hoffmann, Sulfonated surfactants obtained from furfural. *Green Chem.* 2013, **15**, 1558-1566.
[20] K. Gollnick and A. Griesbeck, Singlet Oxygen Photooxygenation of Furans Isolation and Reactions of (4+2)-Cycloaddition Products (unsaturated sec.-Ozonides). *Tetrahedron* 1985, **41**, 2057-2068. T. Montagnon, D. Noutsias, I. Alexopoulou, T. Tofi and G. Vassilikogiannakis, Green oxidations of furans – initiated by molecular oxygen – that give key natural product motifs. *Org. Biomol. Chem.* 2011, **9**, 2031-2039.
[21] C. Escobar, F. Fariña and J. M. Sañudo, Pseudoésteres y derivados III. Pseudoésteres 3-formilacrílicos monohalogenados. Preparatión, estructura y comportamiento en la síntesis diénica. *An. Quim.* 1971, **67**, 43-57. F. Fariña, M. R. Martín and M. V. Martín, Pseudoésteres y derivados XI. Síntesis y estructura de derivados de los ácidos 2-bromo- y 2-cloro-4-oxo-2-butenoicos. *An. Quim.* 1979, **75**, 144-149.
[22] L. Vasamsetty, F. A. Khan and G. Mehta, Total synthesis of a novel oxa-bowl natural product paracaseolide A via a 'putative' biomimetic pathway. *Tetrahedron Lett.* 2013, **54**, 3522-3525. Q. Pei, J. Sun, C. Jin, M. Niu and K. Huang,

Synthesis, Stereochemistry and Anti-cancer Activity of 6-N-Alkyl-4-methoxy-3-oxa-6-aza-bicyclo[3.1.0]hexan-2-one. *Chin. J. Org. Chem.* 2010, **30**, 698-702. H. Huan and Q. Chen, Synthesis of enantiomerically pure spiro-cyclopropane derivatives containing multichiral centers. *Tetrahedron Asymm.* 1998, **9**, 4103-4107.
[23] B. Ciubini, S. Visentin, L. Serpe, R. Canaparo, A. Fin and N. Barbero, Design And Synthesis of Symmetrical Pentamethine Cyanine Dyes As NIR Photosensitizers For PDT. *Dyes Pigm.* 2019, **160**, 806-813.
[24] For further examples of different compound families see: A. Levitz, F. Marmarchi and M. Henary, Synthesis and Optical Properties of Near-Infrared meso-Phenyl-Substituted Symmetric Heptamethine Cyanine Dyes. *Molecules* 2018, **23**, 226. V. A. Svetlichniyĭ, O. K. Bazyl', V. Ya. Artyukhov, T. N. Kopylova, N. A. Derevyanko and A. A. Ishchenko, Specific Features of the Two-Photon Absorption of Cationic Symmetric Polymethine Dyes. *Opt. Spectrosc.* 2007, **103**, 753-760. E. D. Cosco, J. R. Caram, O. T. Bruns, D. Franke, R. A. Day, E. P. Farr, M. G. Bawendi and E. M. Sletten, Flavylium Polymethine Fluorophors for Near- and Shortwave Infrared Imaging. *Angew. Chem. Int. Ed.* 2017, **56**, 13126-13129.
[25] H. Mustroph and A. Towns, Fine Structure in Electronic Spectra of Cyanine Dyes: Are Sub-Bands Largely determined by a Dominant Vibration of a Collection of Singly Excited Vibrations?. *ChemPhysChem*, 2018, **19**, 1016-1023. H. Mustroph, Merocyanine dyes. *Phys. Sc. Reviews*, 2020, 20190145.
[26] R. S. Lepkowicz , O. V. Przhonska, J. M. Hales, J. Fu, D. J. Hagan, E. W. Van Stryland, M. V. Bondar, Y. L. Slominsky and A. D. Kachkovski, Nature of the electronic transitions in thiacarbocyanines with a long polymethine chain. Chem. Phys. 2004, 305, 259–270. S. Pascal, S.-H. Chi, J. W. Perry, C. Andraud and O. Maury, Impact of Ion-Pairing Effects on Linear and Nonlinear Photophysical Properties of Polymethine Dyes. *ChemPhysChem*, 2020, **21**, 2536-2542.
[27]M. Guillaume, B. Champagne and F. Zutterman, Investigation Of The UV/Visible Absorption Spectra of Merocyanine Dyes Using Time-Dependent Density Functional Theory. *J. Phys. Chem. A* 2006, **110**, 13007-13013.
[28] J. Haenle, K. Bruchlos, S. Ludwigs, A. Köhn and S. Laschat, Rigidified Push-Pull Dyes: Using Chromophore Size, Donor, and Acceptor Units to Tune the Ground State Between Neutral and the Cyanine Limit. *ChemPlusChem* 2017, **82**, 1197-1210.
[29] J. H. Dymond, Solubility of a series of gases in cyclohexane and dimethylsulfoxide. *J. Phys. Chem*., 1967, **71**, 1829-1831.
[30] P. Wang, F. Qin, Z. Zhang and W. Cao, Quantitative monitoring of the level of singlet oxygen using luminescence spectra of photophorescent photosenistizer *Optics express* 2015, **23**, 22991-23003.
[31] A. C. Benniston and A. Harriman, Photoinduced and Thermal Isomerization Processes for Bis-Oxonols: Rotor Volume, Stereochemical and Viscosity Effects. *J. Chem. Soc. Faraday Trans.* 1994, **90**, 2627-2634.
[32] A. D. Laurent and D. Jacquemin, TD-DFT benchmarks: A review. *Int. J. Quantum Chem.* 2013, **113**, 2019–2039. F. Muniz-Miranda, A. Pedone, G. Battistelli, M. Montalti, J. Bloino and V. Barone, Benchmarking TD-TFT against Vibrationally Resolved Absorption Spectra at Room Temperature: 7-Aminocoumarins as Test Cases. *J. Chem. Theory Comput.* 2015, **11**, 5371-5384.
[33] S. Botsi and A. Tsolomitis, One or two step acid mediated cyclocondensation process for the preparation of 5-carbethox-2-thiouracils from diethyl ethoxymethylenemalonate an thioureas. *Heterocyclic Com.* 2007, **13**, 229-234.
[34] J. Figueiredo, J. L. Serrano, E. Cavalheiro, L. Keurulainen J. Yli-Kauhaluoma, V. M. Moreira, S. Ferreira, F. C. Domingues, S. Silvestre and P. Almeida, Trisubstituted barbiturates and thiobarbiturates: Synthesis and biological evaluation as xanthine oxidase inhibitors, antioxidants, antibacterial and anti-proliferative agents. *Eur. J. of Med. Chem.* 2018, **143**, 829-842.
[35] M. J. Frisch, et al. *Gaussian 09, Revision D.01*; Gaussian, Inc.: Wallingford, CT, USA, 2010.
[36] C. Lee, W. Yang and R. G. Parr, Development of the Colle-Salvetti correlation-energy formula into a functional of the electron density. *Phys Rev. B* 1988, **37**, 785-789.
[37] J. Tirado-Rives and W. L. Jorgensen, Performance B3LYP Density Functional Methods for a Large Set of Organic Molecules. *J. Chem. Theory Comput.* 2008, **4**, 297-306. K. C. Kreß, T. Fischer, J. Stumpe, W. Frey, M. Raith, O. Beiraghi, H. Eichhorn, S. Tussetschläger and S. Laschat, Influence of Chromophore Length and Acceptor Groups on the Optical Properties of Rigified Merocyanine Dyes. *ChemPlusChem* 2014, **79**, 223-232. R. Berraud-Pache, E. Santamaria-Aranda, B. de Souza, G. Bistoni, F. Neese, D. Sampedro and R. Izsák, Redesigning donor-acceptor Stenhouse adduct photoswitches through a joint experimental and computational study. *Chem. Sci.* 2021, **12**, 2916-2924.
[38] S. Grimme, S. Ehrlich and L. Goerigk, Effect of the Damping Function in Dispersion Corrected Density Functional Theory. *J. Comp. Chem.* 2011, **32**, 1456-1465.

[39] J. Tomasi, B. Mennucci and R. Cammi, Quantum Mechanical Continuum Solvation Models. *Chem. Rev.* 2005, **105**, 2999-3093.
[40] M. Fortino, J. Bloino, E. Collini, L. Bolzonello, M. Trapani, F. Faglioni and A. Pedone, On the simulation of vibrationally resolved electronic spectra of medium-size molecules: the case of styryl substituted BODIPYs. *Phys. Chem. Chem. Phys.* 2019, **21**, 3512-3526. J. Bloino, M. Biczysko, F. Santoro and V. Barone, General Approach to Compute Vibrationally Resolved One-Photon Electronic Spectra. *J. Chem. Theory Comput.* 2010, **6**, 1256-1274.

GRAPHICAL ABSTRACT
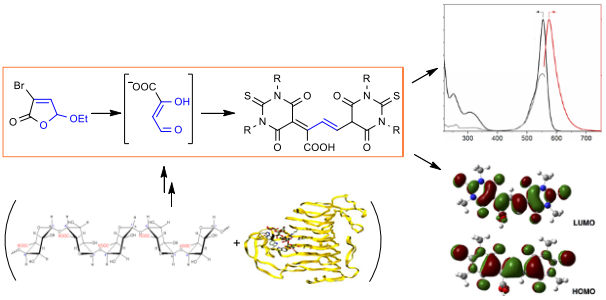
Polymethine dyes are prepared using a convenient synthesis and characterized by physicochemical and computational methods.